



High-surface-area tofu based activated porous carbon for electrical double-layer capacitors



Do-Young Lee^a, Geon-Hyoung An^b, **Hyo-Jin Ahn^{a,b,*}**

^a Department of Materials Science and Engineering, Seoul National University of Science and Technology, Seoul 139-743, Republic of Korea

^b Program of Materials Science & Engineering, Convergence Institute of Biomedical Engineering and Biomaterials, Seoul National University of Science and Technology, Seoul 139-743, Republic of Korea

ARTICLE INFO

Article history:

Received 10 February 2017

Received in revised form 14 March 2017

Accepted 18 March 2017

Available online 27 March 2017

Keywords:

Electrical double layer capacitors

Activated porous carbon

Tofu

Surface area

Wettability

ABSTRACT

Activated porous carbon (APC), which is used as the electrode material in electrical double layer capacitors (EDLCs), is constantly being developed to enhance its electrochemical performance with low cost. Nevertheless, APC still encounters important challenges due to the limited amount of raw material resources. Herein, we propose a novel and simple approach to synthesize APC from tofu using a simple synthesis process involving carbonization with KOH activation. To obtain the optimized APC, three types of APCs are prepared using different weight ratios of 1:3, 1:4, and 1:5 ($W_{\text{Tofu}}/W_{\text{KOH}}$) during the carbonization. The optimized APC electrode shows an outstanding specific capacitance of 207 F g^{-1} at a current density of 0.1 A g^{-1} , a remarkable high-rate performance, an impressive energy density of $25.7\text{--}19.9 \text{ Wh kg}^{-1}$, and an excellent cycling stability for up to 2000 cycles. Therefore, this unique approach to obtain APC using tofu yield a material with some useful qualities in terms of an increased number of electroactive sites based on a high surface area, and an improved wettability based on the oxygen-containing functional groups on the surface of the APC. Accordingly, tofu-based APC is a promising alternative to conventional APC.

© 2017 The Korean Society of Industrial and Engineering Chemistry. Published by Elsevier B.V. All rights reserved.

Introduction

The development of high-performance energy storage devices is of great importance to the advancement of eco-friendly and renewable energy [1]. Among the various energy storage devices, electrochemical capacitors (ECs) have attracted extensive attention because of their high power density, fast energy-storage rate, long life cycle, and wide range of operating temperatures, as compared with conventional secondary batteries [2–4]. Consequently, ECs are being gradually used in applications such as electric vehicles, portable electronic devices, and large-scale industrial equipment [2–4].

In general, ECs are divided into three types according to their energy-storage mechanism. The first type of EC includes electrical double-layer capacitors (EDLC) that are based on a capacitive (non-Faradaic) process by the accumulation of electrostatic

charges between the carbon-based electrode and electrolyte [5,6]. The second type includes pseudo-capacitors based on a redox reaction (Faradaic) process involving reversible electron-exchange reactions between the metal-oxide and/or redox polymer-based electrode and the electrolyte [5,6]. Finally, the third type of ECs are hybrid capacitors, which are based on a mixed reaction that consists of non-Faradaic processes brought about by the accumulation of electrostatic charges at the carbon-based electrode, and Faradaic processes based on reversible electron-exchange reactions on the metal oxide-based electrode [6]. Among ECs, EDLCs have been mostly employed in industrial sites due to their high power density, outstanding cycling stability, and high-rate performance, as compared with pseudo and hybrid capacitors [7–10]. However, EDLCs that use carbon-based electrode materials still suffer serious challenges such as a low energy density. In other words, the energy storage performance of EDLCs is mainly determined by the carbon-based electrode. Thus, there is a crucial need to develop advanced carbon materials with improved properties such as a high specific surface area and wettability, using simple synthesis processes.

Activated porous carbon (APC) is mostly used as the electrode material of commercial EDLCs because of its high surface area,

* Corresponding author at: Department of Materials Science and Engineering, Seoul National University of Science and Technology, Seoul 139-743, Republic of Korea.

E-mail address: hjahn@seoultech.ac.kr (H.-J. Ahn).

chemical stability, and environmental friendliness [11–14]. Nevertheless, to improve the capacitance of EDLCs, it is still a requirement for APCs to have an increased surface area. In addition, the wettability of APC is one of the key issues for the high-rate performance of EDLCs. One way to improve the wettability of APC is to endow its surface with oxygen-containing functional groups, resulting in efficient utilization of surface area, and leading to enhanced capacitance at high current densities. Thus, advanced research for the optimization of APC with high a surface area and excellent wettability is still needed.

Tofu can be used as the raw material for the fabrication of APCs owing to its high porosity (~85%). Tofu, which is derived from soybeans, is composed of proteins, water, and fat. As a food has become increasingly popular all over the world because it is cholesterol free, and contains many nutrients such as minerals, omega-3 fatty acids, vitamins, and isoflavone [15,16]. Herein, APC was derived from tofu using a simple approach that included its carbonization through KOH activation because the tofu has abundant raw materials, porous structure, low-cost, and nitrogen-containing [17]. From the results, it was found that the APC porous structure, with its high-surface area, could be easily controlled by the KOH activation using different tofu-to-KOH weight ratios of 1:3, 1:4, and 1:5 ($W_{\text{Tofu}}/W_{\text{KOH}}$). Furthermore, the KOH activation promoted the formation of oxygen-containing functional groups on the surface of the APC, leading to its improved wettability. The optimized APC indicated unique material characteristics with a higher surface area and improved wettability. As a result, APC-based EDLCs demonstrated an excellent electrochemical performance with a high specific capacitance, high specific energy density, and superb cyclic stability.

Experimental

Chemicals

Tofu was purchased from Pulmuone Co., Ltd. (Korea). Potassium hydroxide (KOH) was purchased from SAMCHUN and it was used without further purification.

Synthesis of the activated porous carbon derived from tofu

Firstly, the tofu was dried in an oven at 80 °C to remove any moisture, and then heated at 400 °C to eliminate impurities. Thereafter, the prepared sample was mixed with KOH, and then carbonized at an activation temperature of 800 °C under a nitrogen atmosphere. Finally, the resultant sample was washed several times with de-ionized water, and dried at 80 °C in an oven. To obtain the optimized APC, three types of samples were prepared using different tofu-to-KOH weight ratios of 1:3, 1:4, and 1:5 ($W_{\text{Tofu}}/W_{\text{KOH}}$), which are hereafter referred to as APC 1:3, APC 1:4, and APC 1:5, respectively. In addition, for comparison purposes, we also prepared carbon derived from tofu without activation using KOH, herein referred to as CDT.

Characterization

The structure and morphology of the APCs were investigated by using field-emission scanning electron microscopy (FESEM), and transmission electron microscopy (MULTI/TEM; Tecnai G², KBSI Gwangju Center). Their crystal structure was examined by X-ray diffractometry (XRD). The chemical bonding states were confirmed by X-ray photoelectron spectroscopy (XPS) using an Al K_α X-ray source. The specific surface area, pore volume, and pore diameter of the APCs were characterized by using Brunauer–Emmett–Teller (BET) and Barrett–Joyner–Halenda (BJH) analyses of N₂ adsorption isotherms (77 K).

Preparation of electrodes and electrochemical characterization

The electrochemical characterization was carried out with a symmetric two-electrode system that used nickel foam (Mtikorea) as the substrate, and a 6M KOH solution as the electrolyte. The electrode was fabricated from a paste slurry, made up of the prepared samples as the active material (70 wt%), polyvinylidene difluoride (20 wt%) as the binder, and Ketjen black as the conducting materials. These were dissolved in *N*-methyl-2-pyrrolidinone (NMP), and thereafter the paste was used to coat

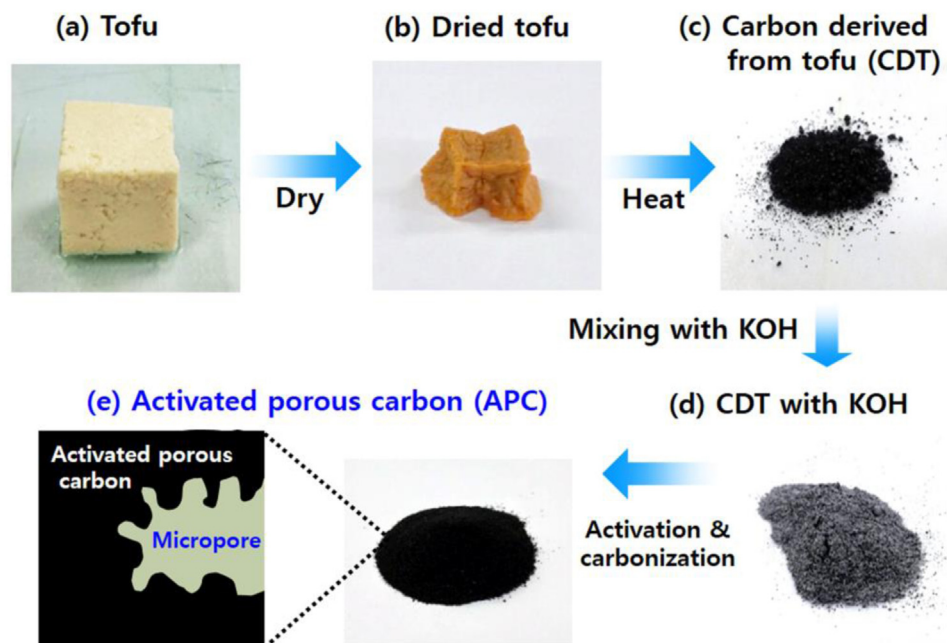


Fig. 1. Illustration of the APC synthesis route. (a) Tofu purchased from Pulmuone. (b) Dried tofu. (c) CDT obtained using a heat-treatment. (d) CDT fabricated with KOH. (e) APC obtained using the carbonization and KOH activation.

a 1-cm² nickel foam. The mass loading of active materials was optimized and fixed with $24.8 \pm 3 \text{ mg cm}^{-2}$. The resultant electrodes were dried at 80 °C for 12 h. Cyclic voltammetry (CV) measurements were performed with a potentiostat/galvanostat (Ecochemie Autolab, PGST302N) in the range of potential 0.0–1.0 V at a scan rate of 10 mV s^{-1} . The charging/discharging tests were carried out at a current density of $0.1\text{--}5.0 \text{ A g}^{-1}$ in the potential range of 0.0–1.0 V using a battery cycle system (WonATech Corp., WMPG 3000). The cycling stability was measured up to 2000 cycles at a current density of 1.0 A g^{-1} .

Results and discussion

Fig. 1 illustrates the ideal preparation process for fabricating APC. The tofu (Fig. 1a) was first dried to dewater it, then it was heated to remove some organic compounds (Fig. 1b), and therefore CDT was formed (Fig. 1c). Finally, to activate the CDT, KOH activation was performed during the carbonization, as shown in Fig. 1d. Three different amounts of KOH were utilized to determine the optimized APC.

Fig. 2a–h presents low-resolution (Fig. 2a–d) and high-resolution (Fig. 2e–h) FESEM images of CDT, APC 1:3, APC 1:4, and APC 1:5. As shown in Fig. 2a and e, CDT with diameters from 5 to 9 μm displayed smooth surfaces without a porous structure. Interestingly, as the relative amount of KOH increased, the amount of pores gradually increased on going from the APC 1:3 (Fig. 2b and f) to the APC 1:4 (Fig. 2c and g) sample, due to the considerable increase in contact area between the KOH and carbon. However, APC 1:5 (Fig. 2d and h) showed large pores due to excessive activation related to the large amounts of KOH utilized. These results indicate that using excess amounts of KOH during carbonization reduced the specific surface area of the carbon materials by reducing the number of pores.

Fig. 3 shows the TEM images of CDT, APC 1:3, APC 1:4, and APC 1:5. All the samples exhibited a uniform contrast over the whole image, which means that these samples consisted of only one phase. CDT (Fig. 3a) displayed a smooth surface structure. It can be clearly seen that as the relative amount of KOH increased, the microporous structure at the surface gradually changed on going from CDT to APC 1:5. The formation of a microporous structure at

the surface of the APC samples was attributed to the KOH activation during the carbonization. It is theorized that the increased microporous structure of APC could improve the electrochemical properties of EDLCs due to the increased number of electroactive sites between the electrode and the electrolyte.

Fig. 4a displays the XRD patterns of the samples, which were used to investigate their crystalline phases and crystallinities. All samples exhibited broad peaks at around 25° corresponding to the (002) layers of graphite [18,19]. In addition, the diffraction peaks of APC 1:4 and APC 1:5 observed at 43.0° and 62.5° , correspond to the (200) and (220) planes, respectively, of face-centered structured MgO (JCPDS card No. 87-0653). During the production of tofu, Mg was used to coagulate the ground soy in water. Thus, APC 1:4 and APC 1:5 have some impurities. The Mg was oxidized to MgO during heating at 400 °C. The MgO phases in APC were stable during the cycling without any electrochemical reactions, as shown in Fig. S1. However, the MgO peaks is not indicated in XRD results of APC 1:3 due to the low amount of KOH activation, leading to relatively low carbon exhaustion. In addition, to investigate the chemical bonding states on the sample surface, XPS measurements were carried out, as shown in Fig. 4b–e. The decomposition of the C1s spectra of all the samples reflect four peaks, namely those of C–C at 284.5 eV, C–O at 285.5 eV, C=O at 286.6 eV, and O–C=O at 288.5 eV. The C–O and C=O peaks correspond to hydroxyl (–OH) groups, and the O–C=O peaks correspond to carboxyl (–COOH) groups [20,21]. Table 1 summarizes the percentages of oxygen-containing functional groups on the surface of the samples. These results demonstrate a development in the number of oxygen-functional groups on the surface of the samples after the KOH activation. In addition, there was an increased number of oxygen-functional groups as the increasing amount of KOH increased. The increased number of oxygen-functional groups on the surface could provide a surpassing high-rate performance of EDLCs, in comparison with carbon–carbon groups, owing to the improved wettability of the electrolyte, which results in the efficient utilization of the surface area, and improved ion transport properties at high current densities [22,23].

To examine the porous characteristic of APC, N₂ adsorption/desorption isotherms were investigated by BET measurements, as shown in Fig. 5a. The isotherms of all samples present type I

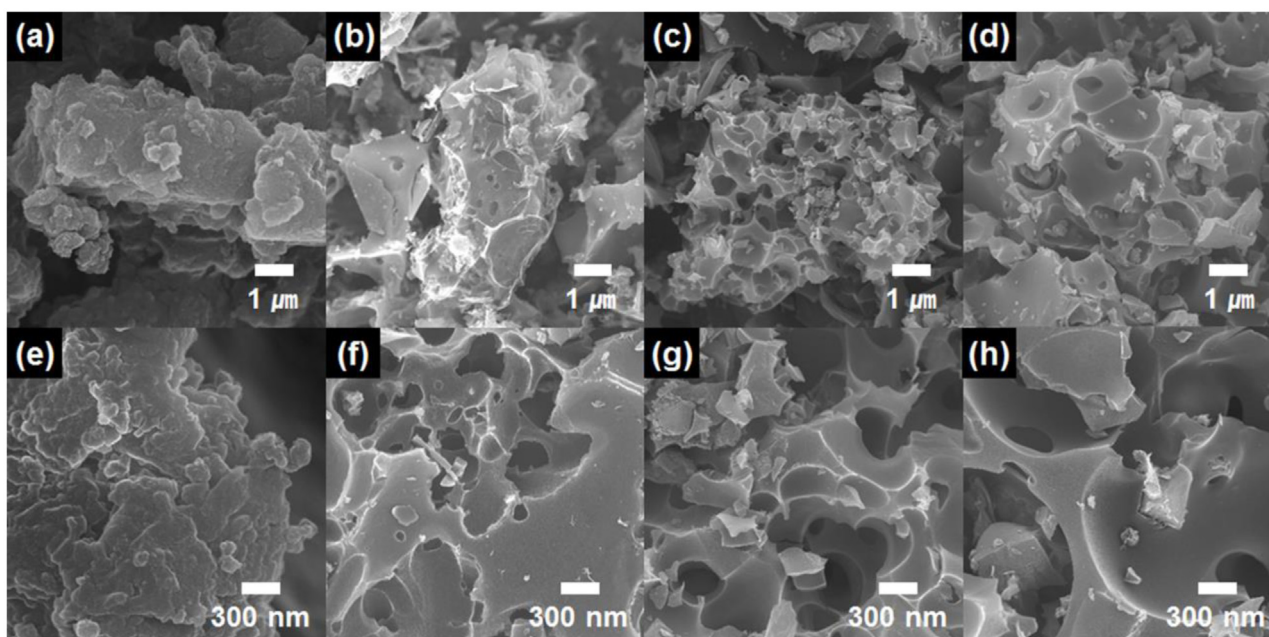


Fig. 2. (a–d) Low-resolution and (e–h) high-resolution FESEM images of the (a and e) CDT, (b and f) APC 1:3, (c and g) APC 1:4, and (d and h) APC 1:5.

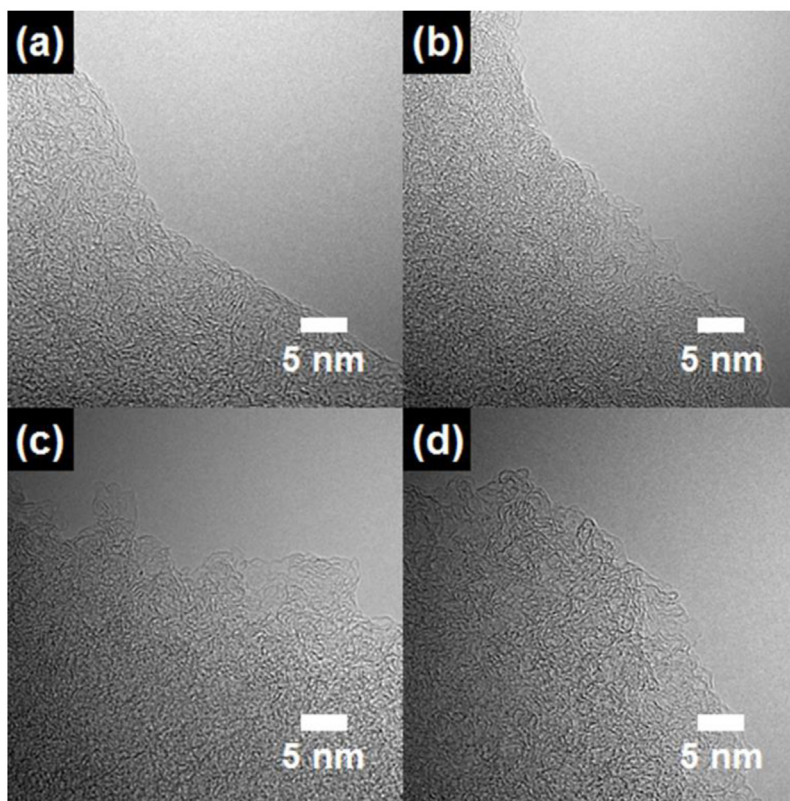


Fig. 3. HRTEM images of the (a) CDT, (b) APC 1:3, (c) APC 1:4, and (d) APC 1:5.

characteristics, which indicate the existence of micropores (pore width < 2 nm) based on the international union of pure and applied chemistry (IUPAC) [24]. The detailed results of the BET measurements including specific surface area, total pore volumes, and average pore diameters are summarized in Table 2. For comparison, commercial APC was purchased from power carbon

technology (PCT), as shown in Fig. S2. The specific surface area of APC 1:4 ($2960 \text{ m}^2 \text{ g}^{-1}$) was higher than that of CDT ($56 \text{ m}^2 \text{ g}^{-1}$), APC 1:3 ($2794 \text{ m}^2 \text{ g}^{-1}$), APC 1:5 ($2444 \text{ m}^2 \text{ g}^{-1}$), and the commercial APC ($2239 \text{ m}^2 \text{ g}^{-1}$) as shown in Fig. S3 and Table S1. These results suggest that the optimized condition for the activation of tofu was a 1:4 weight ratio of tofu-to-KOH. However, the specific surface

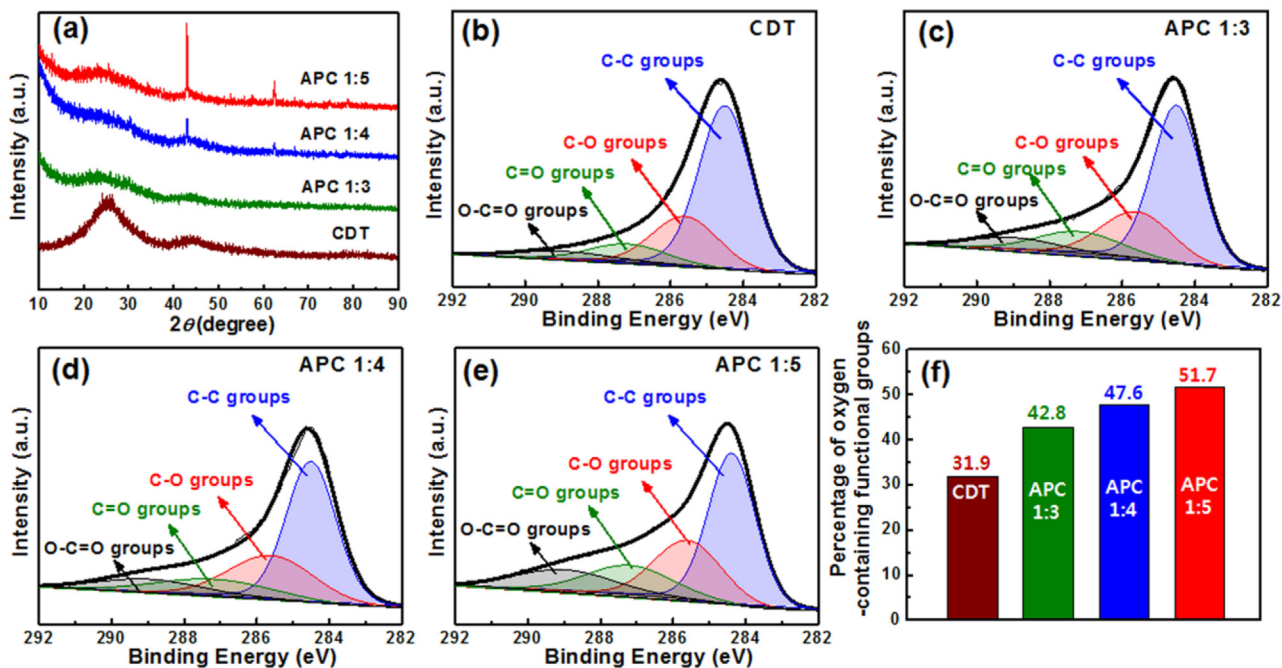
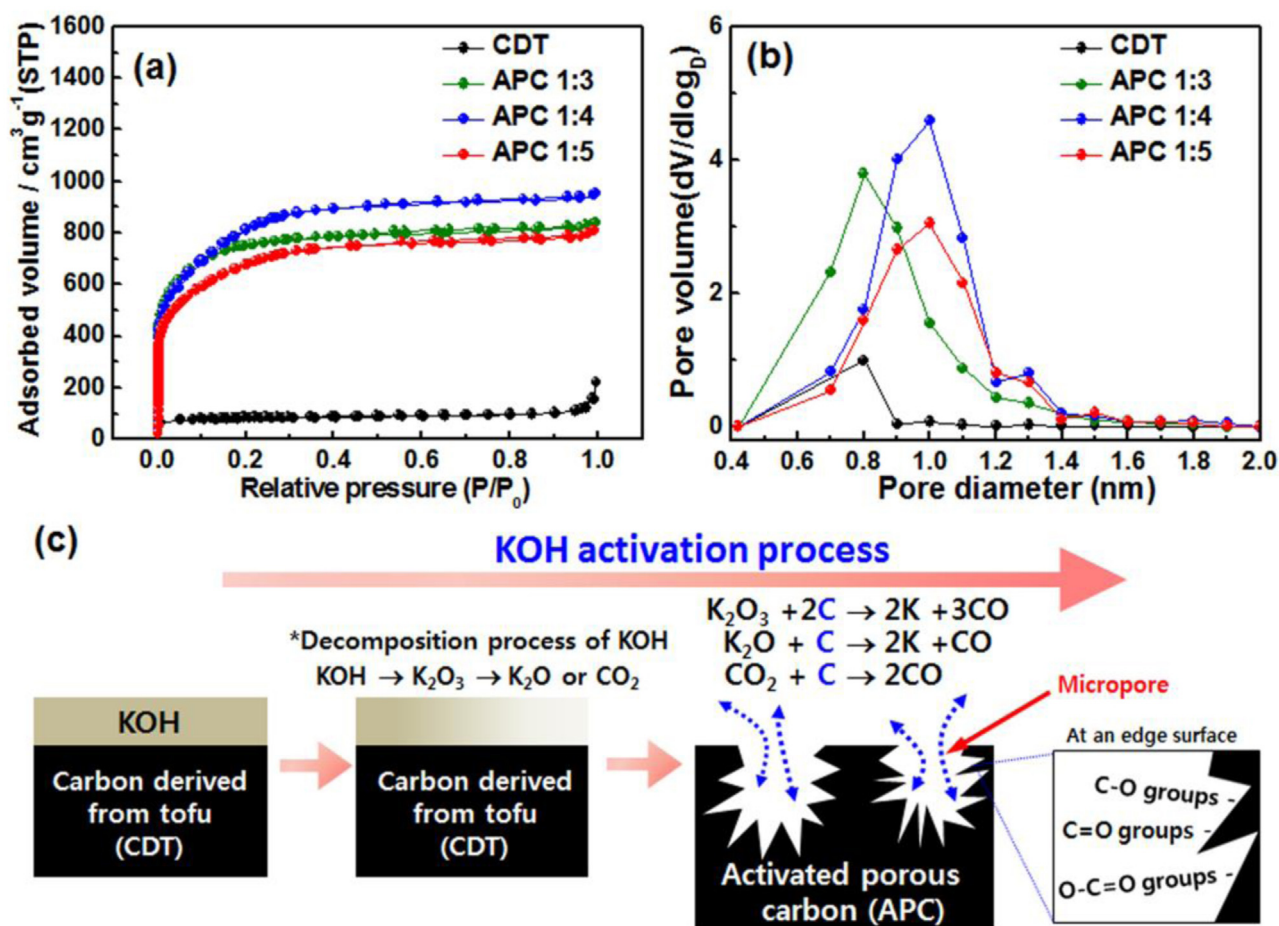


Fig. 4. (a) XRD patterns of CDT, APC 1:3, APC 1:4, and APC 1:5. XPS spectra of C1s of (b) CDT, (c) APC 1:3, (d) APC 1:4 and (e) APC 1:5. (f) Percentage of oxygen-containing functional groups in the XPS spectra of C1s.

Table 1

Percentages of oxygen-containing functional groups on the surface of CDT, APC 1:3, APC 1:4, and APC 1:5.

Samples	C—C (284.5 eV ± 0.3 eV)	C—O (286.0 eV ± 0.3 eV)	C=O (287.4 eV ± 0.3 eV)	O—C=O (288.9 eV ± 0.3 eV)
CDT	63.1	22.5	9.4	5
APC 1:3	57.2	23.1	12.6	7.1
APC 1:4	52.4	25.7	12.8	9.1
APC 1:5	48.1	25.2	13.1	13.4

**Fig. 5.** (a) N₂ adsorption/desorption isotherms and (b) BJH pore size distributions of CDT, APC 1:3, APC 1:4, and APC 1:5. (c) Schematic illustration of the KOH activation process of APC.

area of APC 1:5 was lower than that of APC 1:4 due to the excessive activation of the tofu-derived carbon, which led to the formation of large pores, as shown in Fig. 2h. In addition, the average pore size dropped from 5.5 nm for CDT, to 1.9 nm for APC 1:4, indicating that KOH activation mainly formed micropores. Fig. 5b shows the pore volumes and pore size distributions obtained with the BJH measurements. The APC 1:4 sample displayed micropores ranging in size from 0.6 to 1.2 nm, which are values in good concurrence with the BET results. Therefore, the development of micropores can

be attributed to the release of pyrolysis gases between the KOH and carbon during the carbonization process with the activation. The activation process can be explained by the following reaction: $\text{KOH} + \text{C} \leftrightarrow \text{K} + \text{H}_2 + \text{K}_2\text{CO}_3$. Thereafter, the decomposition of K_2CO_3 to K_2O , and CO_2 lead to the activation with tofu-derived carbon [25,26]. After activation, the porous high specific surface area of APC 1:4 played a key role in obtaining a high specific capacity due to the large number of electroactive sites between the electrode and electrolyte [27,28].

Table 2

List of a specific surface area, pore volume, and average pore diameter of CDT, APC 1:3, APC 1:4, and APC 1:5.

Samples	S _{BET} (m ² g ⁻¹)	Total pore volume (p/p ₀ =0.990) (cm ³ g ⁻¹)	Average pore diameter (nm)
CDT	56	0.077	5.51
APC 1:3	2794	1.29	1.84
APC 1:4	2960	1.47	1.98
APC 1:5	2444	1.25	2.05

To investigate the electrochemical behavior of the electrodes, CV measurements were carried out using a potentiostat/galvanostat in the potential range of 0.0–1.0 V at a scan rate of 10 mV s^{-1} , in an aqueous 6 M KOH electrolyte, as shown in Fig. 6a. The APC 1:4 electrode displayed the largest rectangular ideal curve, which means that the electrical double-layer area, which resulted from the high specific surface area consisting of the micropores, was increased. The specific capacitance (C_{sp}) of the electrodes was calculated at a current density of $0.1\text{--}5.0 \text{ A g}^{-1}$ according to the following equation [29–31]:

$$C_{sp} = 4I/(m dV/dt) \quad (1)$$

where I (A) is the applied current, m (g) is the total mass of the active material, dV is the voltage drop, and dt (s) is the discharging time. The specific capacitances of CDT, APC 1:3, APC 1:4, APC 1:5 and commercial APC electrodes were 58, 160, 207, 157, and 168 F g^{-1} , respectively, at a current density of 0.1 A g^{-1} , as shown in Fig. 6b. The CDT electrode showed the lowest specific capacitance, in comparison with the other electrodes, due to its non-porous structure with low specific surface area. After the activation, the electrodes exhibited an increased specific capacitance, implying the improvement of the electrode's surface. The APC 1:4 electrode exhibited an impressive specific capacitance at all current densities, in comparison with the other electrodes and the commercial APC electrode. The improved specific capacitance of the APC 1:4 electrode was ascribed to its high specific surface area, compared with the other samples and the large number of oxygen-containing functional groups on its surface. However, the commercial APC exhibited a relatively low specific

capacitance due to its lower specific surface area. In addition, the APC 1:5 electrode, which had a low specific surface area, showed a relatively low specific capacitance compared to the APC 1:4 sample due to the excessive KOH activation of APC 1:5. Therefore, the specific surface area is a very important factor for improving the specific capacitance compared to oxygen-containing functional groups. Moreover, the specific capacitances of all the electrodes were reduced slightly as the current density was increased due to a reduced ion diffusion time during the cycling process. Nonetheless, the APC 1:4 electrode presented an outstanding high-rate performance with a capacitance retention of 81% due to its improved wettability springing from the increased number of oxygen-containing functional groups on its surface. However, the commercial APC, which had a fewer number of oxygen-containing functional groups of only 39.6% (Fig. S4 and Table S2), showed a relatively poor high-rate performance at a current density of 5.0 A g^{-1} . These results can be explained by the fact that at high current densities an improved wettability is easily accessible to the ions, leading to the enhanced high-rate performance.

In the Ragone plot (Fig. 6c), the energy density (E , Wh kg^{-1}) and power density (P , W kg^{-1}) are evaluated on the basis of charge/discharge tests using a two-electrode system by the following equation [19,23,32]:

$$E = C_{sp} V^2 / 8 \quad (2)$$

$$P = E / dt \quad (3)$$

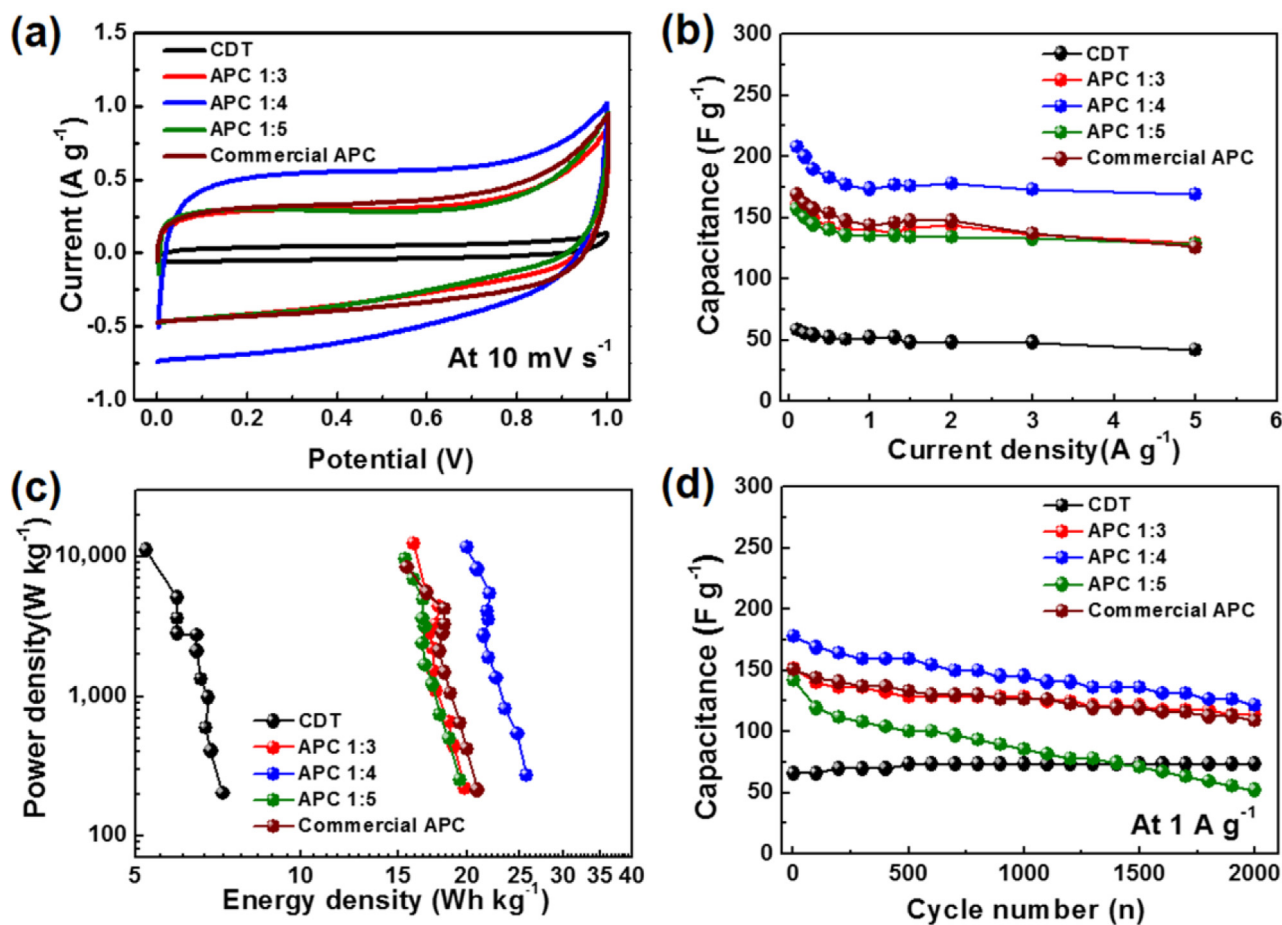


Fig. 6. (a) CV measurements of CDT, APC 1:3, APC 1:4, APC 1:5, and commercial APC electrodes at a scan rate of 10 mV s^{-1} in a voltage range of 0.0–1.0 V. (b) Specific capacitance at a current density of $0.1\text{--}5.0 \text{ A g}^{-1}$. (c) Ragone plot in the power density range from $272.1\text{--}11,694.3 \text{ W kg}^{-1}$. (d) Cycling stability at a current density of 1 A g^{-1} up to 2000 cycles.

where V is the discharging voltage, and dt is the total discharge time. The Ragone plots display a decrease in the energy density as the power density increases. In comparison with the other electrodes, the APC 1:4 sample exhibited the highest energy density value of 25.7–19.9 Wh kg⁻¹, in the power density range of 272.1–11,694.3 W h kg⁻¹. Fig. 6d displays the cycling stability of all the electrodes evaluated at a current density of 1.0 A g⁻¹ for up to 2000 cycles. The APC 1:4 electrode had an excellent cycling stability with a specific capacitance of 170 F g⁻¹ after 2000 cycles. However, the APC 1:5 electrode with larger pores showed a poor cycling stability with a specific capacitance of 128 F g⁻¹ after 2000 cycles. Thus, the larger pore diameters of APC reduced the specific capacitance due to its detachment of the active materials, leading to the poor cycling stability [33,34].

Thus, the remarkable electrochemical performance of the APC 1:4 electrode can be ascribed to two major effects. Firstly, a high surface area can provide an increased number of electroactive sites between the electrode and the electrolyte, thus increasing the capacitance. Secondly, the increased number of oxygen-containing functional groups on the surface of the electrode improves its wettability, leading to its outstanding high-rate performance.

In addition, the cost of commercial APCs is very expensive due to the limited amount of raw materials from which they are made, such as coals, petroleum cokes, and tar pitches. Furthermore, the prices of APCs are increasing owing to their various applications, which include gas adsorbents and water filters. Therefore, APCs derived from tofu can be a good option to reduce the production costs owing to the lower cost of the raw material.

Conclusions

APC derived from tofu was successfully synthesized through carbonization with KOH activation. The optimized APC 1:4 sample showed a microporous structure with a high specific surface area of 2960 m² g⁻¹, a total pore volume of 1.47 cm³ g⁻¹, and an average pore diameter of 1.9 nm. The microporous structure mainly resulted from the KOH activation. In addition, the amount of oxygen-containing functional groups on the surface of the APC 1:4 sample was to 47.6% after the KOH activation. The APC 1:4 electrode showed a remarkable specific capacitance of 207 F g⁻¹ at a current density of 0.1 A g⁻¹, an outstanding high-rate performance, excellent energy density of 25.7–19.9 Wh kg⁻¹, and impressive cycling stability for up to 2000 cycles. Thus, the notable electrochemical performance of APC 1:4 can be explained in terms of two major factors: (I) its improved specific capacitance, which is related to the increased number of electroactive sites based on its high surface area, and (II) its outstanding high-rate performance related to its improved wettability due to the existence of oxygen-containing functional groups on its surface, which promote the efficient utilization of its surface area. Thus, tofu-derived APC 1:4 has enhanced electrochemical properties

that make it a promising electrode material for its use in low-cost and high-performance ECs.

Acknowledgment

This research was supported by Basic Science Research Program through the National Research Foundation of Korea (NRF) funded by the Ministry of Science, ICT and Future Planning (NRF-2015R1A1A1A05001252).

Appendix A. Supplementary data

Supplementary data associated with this article can be found, in the online version, at <http://dx.doi.org/10.1016/j.jiec.2017.03.032>.

References

- [1] P. Simon, Y. Gogotsi, *Nat. Mater.* 7 (11) (2008) 845.
- [2] N.P.S. Chauhan, M. Mozafari, N.S. Chundawat, K. Meghwal, R. Ameta, S.C. Ameta, *J. Ind. Eng. Chem.* 36 (2016) 13.
- [3] J. Choi, N.R. Kim, H.-J. Jin, Y.S. Yun, *J. Ind. Eng. Chem.* 42 (2016) 158.
- [4] M. Inagaki, H. Konno, O. Tanaiki, *J. Power Sources* 195 (2010) 7880.
- [5] G.-H. An, H.-J. Ahn, *ECS Solid State Lett.* 2 (5) (2013) M33.
- [6] G. Yu, X. Xie, L. Pan, Z. Bao, Y. Cui, *Nano Energy* 2 (2013) 213.
- [7] H.J. An, N.R. Kim, M.Y. Song, Y.S. Yun, H.-J. Jin, *J. Ind. Eng. Chem.* 45 (2017) 223.
- [8] C. Long, L. Jiang, X. Wu, Y. Jiang, D. Yang, C. Wang, T. Wei, Z. Fan, *Carbon* 93 (2015) 412.
- [9] S. Ye, L. Zhu, I.-J. Kim, S.-H. Yang, W.-C. Oh, *J. Ind. Eng. Chem.* 42 (2016) 53.
- [10] G.-H. An, H.-J. Ahn, *Carbon* 65 (2013) 87.
- [11] Y. Zhao, W. Ran, J. He, Y. Song, C. Zhang, D.-B. Xiong, F. Gao, J. Wu, Y. Xia, *ACS Appl. Mater. Interfaces* 7 (2015) 1132.
- [12] R. Madhu, V. Veeramani, S.-M. Chen, P. Veerakumar, S.B. Liu, N. Miyamoto, *Phys. Chem. Chem. Phys.* 18 (2016) 16466.
- [13] X. Deng, B. Zhao, L. Zhu, Z. Shao, *Carbon* 93 (2015) 48.
- [14] J. Hou, C. Cao, F. Idrees, X. Ma, *ACS Nano* 9 (3) (2015) 2556.
- [15] F. Rossi, G.E. Felis, A. Martinelli, B. Calcavecchia, S. Torriani, *LWT Food Sci. Technol.* 70 (2016) 280.
- [16] Q. Zhu, F. Wu, M. Saito, E. Tatsumi, L. Yin, *Food Chem.* 201 (2016) 197.
- [17] T. Ouyang, K. Cheng, Y. Gao, S. Kong, K. Ye, G. Wang, D. Cao, *J. Mater. Chem. A* 4 (2016) 9832.
- [18] G.-H. An, H.-J. Ahn, *J. Power Sources* 272 (2014) 828.
- [19] G.-H. An, E.-H. Lee, H.-J. Ahn, *J. Alloys Compd.* 682 (2016) 746.
- [20] G.-H. An, H.-J. Ahn, *J. Electroanal. Chem.* 744 (2015) 32.
- [21] G.-H. An, D.-Y. Lee, H.-J. Ahn, *ACS Appl. Mater. Interfaces* 8 (2016) 19466.
- [22] Q. Li, R. Jiang, Y. Dou, Z. Wu, T. Huang, D. Feng, J. Yang, A. Yu, D. Zhao, *Carbon* 49 (2011) 1248.
- [23] J.-W. Lang, X.-B. Yan, W.-W. Liu, R.-T. Wang, Q.-J. Xue, *J. Power Sources* 204 (2012) 220.
- [24] G.-H. An, B.-R. Koo, H.-J. Ahn, *Phys. Chem. Chem. Phys.* 18 (2016) 6587.
- [25] J. Wang, S. Kaskel, *J. Mater. Chem.* 22 (2012) 23710.
- [26] Y. Ji, T. Li, L. Zhu, X. Wang, Q. Lin, *Appl. Surf. Sci.* 254 (2007) 506.
- [27] J.E. Zuliani, J.N. Caguiat, D.W. Kirk, C.Q. Jia, *J. Power Sources* 290 (2015) 136.
- [28] B.E. Wilson, S. He, K. Buffington, S. Rudistill, W.H. Smyrl, A. Stein, *J. Power Sources* 298 (2015) 193.
- [29] X. Li, W. Xing, S. Zhuo, J. Zhou, F. Li, S.-Z. Qiao, G.-Q. Lu, *Bioresour. Technol.* 102 (2011) 1118.
- [30] M. Liu, W.W. Tjui, J. Pan, C. Zhang, W. Gao, T. Liu, *Nanoscale* 6 (2014) 4233.
- [31] J. Yang, M.R. Jo, M. Kang, Y.S. Huh, H. Jung, Y.-M. Kang, *Carbon* 73 (2014) 106.
- [32] X. Yang, L. Zhang, F. Zhang, T. Zhang, Y. Huang, Y. Chen, *Carbon* 72 (2014) 381.
- [33] L. Yin, Y. Chen, D. Li, X. Zhao, B. Hou, B. Cao, *Mater. Des.* 111 (2016) 44.
- [34] C. Zhao, F. Ren, X. Xue, W. Zheng, X. Wang, L. Chang, *J. Electroanal. Chem.* 782 (2016) 98.